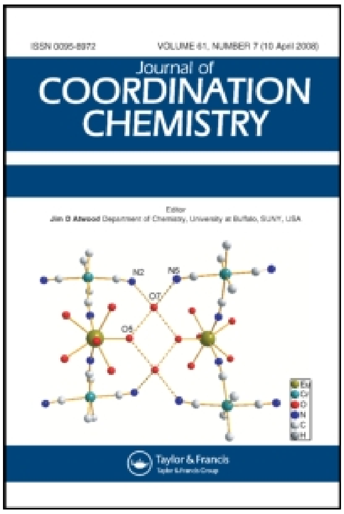

Journal of Coordination Chemistry

Publication details, including instructions for authors and subscription information:
http://www.informaworld.com/smpp/title~content=t713455674

Supramolecular interactions in high molecular weight bisdithiocarbamate adducts of divalent Zn(II), Cd(II), and Hg(II): spectral, VBS, and single crystal X-ray structural studies on MS_4N_2 chromophores

K. Ramalingam[a]; S. Uma[a]; C. Rizzoli[b]; G. Marimuthu[a]
[a] Department of Chemistry, Annamalai University, Annamalainagar - 608 002, India [b] Department of General and Inorganic Chemistry, University of Parma, Parma - 43100, Italy

To cite this Article Ramalingam, K. , Uma, S. , Rizzoli, C. and Marimuthu, G.(2010) 'Supramolecular interactions in high molecular weight bisdithiocarbamate adducts of divalent Zn(II), Cd(II), and Hg(II): spectral, VBS, and single crystal X-ray structural studies on MS_4N_2 chromophores', Journal of Coordination Chemistry, 63: 23, 4123 — 4135, First published on: 29 October 2010 (iFirst)

To link to this Article: DOI: 10.1080/00958972.2010.528409

URL: http://dx.doi.org/10.1080/00958972.2010.528409

Journal of Coordination Chemistry
Vol. 63, No. 23, 10 December 2010, 4123–4135

Taylor & Francis
Taylor & Francis Group

Supramolecular interactions in high molecular weight bisdithiocarbamate adducts of divalent Zn(II), Cd(II), and Hg(II): spectral, VBS, and single crystal X-ray structural studies on MS_4N_2 chromophores

K. RAMALINGAM*†, S. UMA†, C. RIZZOLI‡ and G. MARIMUTHU†

†Department of Chemistry, Annamalai University, Annamalainagar – 608 002, India
‡Department of General and Inorganic Chemistry, University of Parma, Parma – 43100, Italy

(*Received 25 May 2010; in final form 1 September 2010*)

This article describes supramolecular interactions induced in a high molecular weight dithiocarbamate, padtc, by its design. Synthesis, spectral studies involving zinc, cadmium and mercury, padtc, and adducts with tmed, such as $[Zn(padtc)_2]$ (**1**), $[Zn(padtc)_2(tmed)] \cdot C_6H_5CH_3 \cdot 0.5(H_2O)$ (**2**), $[Cd(padtc)_2]$ (**3**), $[Cd(padtc)_2(tmed)] \cdot C_6H_5CH_3 \cdot 0.36(H_2O)$ (**4**), $[Hg(padtc)_2] \cdot H_2O$ (**5**), $[Hg(padtc)_2(2,2'\text{-bipy})] \cdot H_2O$ (**6**), $[Hg(padtc)_2(1,10\text{-phen})] \cdot H_2O$ (**7**), and $[Hg(padtc)_2(oxine)] \cdot H_2O$ (**8**) (where $padtc^- = N,N'$-(iminodiethylene)bisphthalimidedithiocarbamate, 1,10-phen = 1,10-phenanthroline, tmed = tetramethylethylenediamine, 2,2′-bipy = 2,2′-bipyridine, oxine = 8-hydroxyquinoline) along with the single crystal X-ray structural analysis of $[Zn(padtc)_2(tmed)] \cdot C_6H_5CH_3 \cdot 0.5(H_2O)$ (**2**) and $[Cd(padtc)_2(tmed)] \cdot C_6H_5CH_3 \cdot 0.36(H_2O)$ (**4**) are reported. All the complexes were characterized by IR, NMR (^1H and ^{13}C), and thermogravimetric study. The IR spectra of the complexes show the contribution of the thioureide form to the structures. In ^{13}C NMR spectra, the most important thioureide ($N^{13}CS_2$) carbon signals are observed at 210–212 ppm. Single crystal X-ray structural analyses of **2** and **4** show the presence of extensive supramolecular interactions stabilizing the solid-state structure. Both zinc and cadmium are in a distorted octahedral environment with MS_4N_2 chromophores. VBS of Zn and Cd are 1.76 and 1.98, respectively, supporting the correctness of the determined structure and the valence of the central metal ions.

Keywords: Dithiocarbamate; Supramolecular; Thioureide; NMR; Thermogravimetry; Single crystal X-ray structure

1. Introduction

Dithiocarbamates of zinc, cadmium, and mercury continue to attract attention for their industrial applications [1, 2] and biological profiles [3, 4]. Recent publications established that cadmium dithiocarbamates are useful precursors to CdS nanowires [5, 6]. Various main group metal dithiolates have been investigated as precursors in metal organic chemical vapor deposition (MOCVD) [7–9]. The affinity of Zn, Cd, and Hg toward sulfur-containing ligands leads to many compounds [10–12]. Studies of intermolecular interactions of supramolecular compounds have been on the rise in the

---

*Corresponding author. Email: krauchem@yahoo.com

Journal of Coordination Chemistry
ISSN 0095-8972 print/ISSN 1029-0389 online
DOI: 10.1080/00958972.2010.528409

last three decades, with weak intermolecular interactions, such as nonclassical hydrogen bonding, π–π interactions, homoatomic, heteroatomic interactions, hydrophobic forces, van der Waals forces, and contribution of electrostatic effects [13]. Mercury forms many strong linear and tetrahedral complexes, unlike zinc and cadmium. Synthesis and structural studies on [Hg(tetds)I_2] (where tetds = tetraethylthiuramdisulfide), by mixing directly tetraethylthiuramdisulfide and HgI_2 in ethanol, show a distorted tetrahedral environment [14]. In this work, a high molecular weight dithiocarbamate (padtc) has been used to form complexes with the metal ions, which can have interesting analytical applications in the form of a chelating agent (figure 1).

The dithiocarbamate has diketo groups, which enhance supramolecular interactions. The aromatic ring of padtc provides an opportunity for π–π interactions. In view of the interest on the ligand and its supramolecular interactions, this article reports the synthesis and characterization of [Zn(padtc)$_2$] (**1**), [Zn(padtc)$_2$(tmed)] · $C_6H_5CH_3 \cdot 0.5H_2O$ (**2**), [Cd(padtc)$_2$] (**3**), [Cd(padtc)$_2$(tmed)] · $C_6H_5CH_3 \cdot 0.36H_2O$ (**4**), [Hg(padtc)$_2$] · H_2O (**5**), [Hg(padtc)$_2$(2,2′-bipy)] · H_2O (**6**), [Hg(padtc)$_2$(1,10-phen)] · H_2O (**7**), and [Hg(padtc)$_2$(oxine)] · H_2O (**8**) (where 1,10-phen = 1,10-phenanthroline, tmed = tetramethylethylenediamine, 2,2′-bipy = 2,2′-bipyridine, oxine = 8-hydroxyquinoline). The single crystal X-ray structures of [Zn(padtc)$_2$(tmed)] · $C_6H_5CH_3 \cdot 0.5H_2O$ (**2**) and [Cd(padtc)$_2$(tmed)] · $C_6H_5CH_3 \cdot 0.36H_2O$ (**4**) have also been included in the article.

2. Experimental

All reagents and solvents were commercially available analytical grade materials and were used as supplied. IR spectra were recorded on an ABB Bomen MB 104 spectrometer (4000–500 cm^{-1}) as KBr pellets. Thermal analysis was carried out on a STA 409 PC thermal sciences instrument. Single crystal X-ray intensity data were collected at ambient temperature (295 K) using graphite monochromated Mo-Kα radiation ($\lambda = 0.71073$ Å) on a Bruker SMART 1000 CCD diffractometer for **2** and **4**. Data for **2** were corrected for absorption using SADABS [15], while those for **4** were corrected using the multi scan technique [16]. All non-hydrogen atoms were refined anisotropically and hydrogens were fixed geometrically. The PLUTO plots were drawn with ORTEP-3 [17].

2.1. *Preparation of N,N′-(iminodiethylene)bisphthalimide (paH)*

Phthalic anhydride (50 g, 0.35 mmol) was dissolved in boiling chloroform (500 mL) and the solution was filtered to remove phthalic acid [18]. To this solution at 50°C,

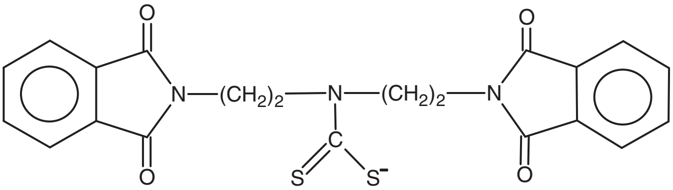

Figure 1. padtc$^-$: *N,N*′-(iminodiethylene)bisphthalimidedithiocarbamate anion.

with stirring, a solution of "dien" in chloroform (16.3 mL, 0.15 mmol) in 100 mL was added slowly (40 min). A white sticky solid precipitated immediately on addition and the solution turned yellow. Most of the chloroform was evaporated and the reaction was completed by heating the mixture at 140°C for 1 h in the oven. The resulting brittle yellow solid was powdered, dissolved in a minimum volume of hot chloroform (250 mL) and was filtered to remove traces of phthalic acid. The yellowish crude product was precipitated with ethanol (500 mL) and was filtered and dried at 100°C. It was recrystallized from hot chloroform containing decolorizing charcoal and precipitated from the filtered solution by the addition of ethanol. The fluffy powder was filtered off, washed with cold ethanol, and dried at 100°C (yield: 60%, dec.: 180°C).

2.2. *Preparation of bis(N,N′-(iminodiethylene)bisphthalimidedithiocarbamato) zinc(II); [Zn(padtc)$_2$] (1)*

Amine, "paH" (0.726 g, 2 mmol) was dissolved in acetonitrile (75 mL), and carbon disulfide (40 mmol, 2.5 mL) was added with continuous stirring; yellow dithiocarbamic acid was obtained. To this, aqueous solution of zinc nitrate hexahydrate (0.297 g, 1 mmol) was added and stirred. The precipitate obtained was filtered, washed with water and acetonitrile, and finally dried in an oven at 100°C. The complex was insoluble in common organic solvents (yield: 60%, dec.: 219°C). Anal. Calcd for $C_{42}H_{32}N_6O_8S_4Zn$ (%): C, 53.52; H, 3.43; N, 8.92. Found (%): C, 53.22; H, 3.09; N, 8.62.

2.3. *Preparation of [Zn(padtc)$_2$(tmed)]$\cdot$$C_6H_5CH_3$$\cdot$0.5($H_2O$) (2)*

A mixture of [Zn(padtc)$_2$] (0.236 g, 0.25 mmol) and tmed (0.377 mL, 0.25 mmol) in toluene–chloroform (1 : 1) solvent mixture (20 mL) was refluxed for an hour. Then the hot clear solution was filtered through filter paper. On cooling, fine yellow transparent crystals were formed (yield: 70%, dec.: 160°C). Anal. Calcd for $C_{55}H_{57}N_8O_{8.50}S_4Zn$ (%): C, 56.92; H, 4.96; N, 9.66. Found (%): C, 56.62; H, 4.61; N, 9.35.

2.4. *Preparation of bis(N,N′-(iminodiethylene)bisphthalimidedithiocarbamato) cadmium(II); [Cd(padtc)$_2$] (3)*

Amine, "paH" (0.7264 g, 2 mmol) was dissolved in acetonitrile (75 mL) and carbon disulfide (40 mmol, 2.5 mL) was added with continuous stirring; yellow dithiocarbamic acid was obtained. To this, aqueous solution of $Cd(NO_3)_2 \cdot 4H_2O$ (0.3085 g, 1 mmol) was added and stirred. The precipitate obtained was filtered, washed with water and acetonitrile, and finally dried in an oven at 100°C. The complex was insoluble in common organic solvents (yield: 60%, dec.: 206°C). Anal. Calcd for $C_{42}H_{32}N_6O_8S_4Cd$ (%): C, 50.98; H, 3.27; N, 8.50. Found (%): C, 50.67; H, 3.07; N, 8.25.

2.5. *Preparation of [Cd(padtc)$_2$(tmed)]$\cdot$$C_6H_5CH_3$$\cdot$0.36($H_2O$) (4)*

A mixture of [Cd(padtc)$_2$] (0.247 g, 0.25 mmol) and tmed (0.377 mL, 0.25 mmol) in toluene–chloroform (1 : 1) solvent mixture (20 mL) was refluxed for an hour. Then the hot solution was filtered off and yellow transparent crystals were obtained by solvent evaporation (yield: 70%, dec.: 170°C). Anal. Calcd for $C_{55}H_{56.72}N_8O_{8.36}S_4Cd$ (%): C, 54.81; H, 4.75; N, 9.30. Found (%): C, 54.47; H, 4.40; N, 9.02.

2.6. *Preparation of bis(N,N′-(iminodiethylene)bisphthalimidedithiocarbamato) mercury(II) monohydrate; [Hg(padtc)$_2$]•H_2O (5)*

Amine, "paH" (0.726 g, 2 mmol) was dissolved in acetonitrile (75 mL), and carbon disulfide (40 mmol, 2.5 mL) was added with continuous stirring; yellow dithiocarbamic acid was obtained. To this, aqueous solution of mercuric chloride (0.2715 g, 1 mmol) was added and stirred well. The dirty white precipitate obtained was filtered, washed with water and acetonitrile, and finally dried in an oven at 100°C. The complex was insoluble in common organic solvents (yield: 60%, dec.: 168°C). Anal. Calcd for $C_{42}H_{34}O_9S_4Hg$ (%): C, 46.03; H, 3.13; N, 7.67. Found (%): C, 45.70; H, 2.98; N, 7.40.

2.7. *Preparation of [Hg(padtc)$_2$(2,2′-bipy)]•H_2O (6)*

A mixture of [Hg(padtc)$_2$] (0.270 g, 0.25 mmol) and 2,2′-bipyridine (0.039 g, 0.25 mmol) in toluene–chloroform (1 : 1) solvent mixture (25 mL) was refluxed for 2 h, followed by concentration to 10 mL. After 2 days, yellow solid separated from the solution. The solid was filtered and dried over anhydrous calcium chloride (yield: 60%, dec.: 64°C). Anal. Calcd for $C_{52}H_{42}N_8O_9S_4Hg$ (%): C, 49.88; H, 3.39; N, 8.96. Found (%): C, 49.52; H, 3.05; N, 8.67.

2.8. *Preparation of [Hg(padtc)$_2$(1,10-phen)]•H_2O (7)*

A mixture of [Hg(padtc)$_2$] (0.270 g, 0.25 mmol) and 1,10-phenanthroline (0.049 g, 0.25 mmol) in toluene–chloroform (1 : 1) solvent mixture (25 mL) was refluxed for 2 h, followed by concentration to 10 mL. After 2 days, yellow solid separated from the solution. The solid was filtered and dried over anhydrous calcium chloride (yield: 60%, dec.: 94°C). Anal. Calcd for $C_{54}H_{52}N_8O_9S_4Hg$ (%): C, 50.82; H, 4.11; N, 8.79. Found (%): C, 50.51; H, 3.91; N, 8.53.

2.9. *Preparation of [Hg(padtc)$_2$(oxine)]•H_2O (8)*

A mixture of [Hg(padtc)$_2$] (0.270 g, 0.25 mmol) and oxine (0.036 g, 0.25 mmol) in toluene–chloroform (1 : 1) solvent mixture (25 mL) was refluxed for 2 h, followed by concentration to 10 mL. After 2 days, yellow solid separated from the solution. The solid was filtered and dried over anhydrous calcium chloride (yield: 60%, dec.: 58°C). Anal. Calcd for $C_{51}H_{41}N_7O_{10}S_4Hg$ (%): C, 49.36; H, 3.34; N, 7.91. Found (%): C, 49.02; H, 3.02; N, 7.71.

3. Results and discussion

A high molecular weight dithiocarbamate, padtc, has been used to form complexes with divalent Zn, Cd, and Hg and their adducts with tmed have been prepared and characterized.

3.1. *IR spectral studies*

IR spectral data of zinc, cadmium, and mercury dithiocarbamates and their adducts are presented in table 1. The reduction in $\nu_{C–N}$ (thioureide) for adducts compared to those observed for their parents is attributed to the change in coordination number from 4 to 6 and also the steric effect exerted by tmed, 2,2′-bipyridine, 1,10-phenanthroline, and oxine. In addition, the observation is an indication of increased electron density on the metal in the adducts. The $\nu_{C–S}$ bands at 956–1043 cm^{-1} for all complexes, with significant split, support the anisobidentate coordination of the dithiocarbamate to the metal center [19, 20]. For the padtc^{-} complexes, an intense band due to 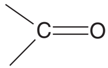 stretch at 1710–1775 cm^{-1} is due to the asymmetrical and symmetrical stretching modes. The carbonyl absorption remains unaffected in the complexes indicating weak supramolecular involvement in complexation. Apart from $\nu_{C–N}$ (thioureide), an intense band around 1395 cm^{-1} is assigned to $\nu_{C–N}$ (tertiary) for padtc complexes, whereas in free "paH" amine and padtc^{-}, $\nu_{C–N}$ (tertiary) are observed at 1394 and 1396 cm^{-1}, respectively. In the complexes, $\nu_{C–H}$ and phenyl C–H vibrations appeared at 2830–3060 and 650–790 cm^{-1}, respectively. The characteristic bands due to 1,10-phenanthroline appear at 1619 and 1504 cm^{-1}. For 2,2′-bipyridine, characteristic aromatic ring vibrations are observed at 1582 cm^{-1} in all its adducts.

3.2. *Thermogravimetric studies*

Thermogravimetric (TG) analysis has been carried out on mercury complexes because all the mercury complexes could not be crystallized. $Hg(padtc)_2 \cdot H_2O$ (**5**) starts to decompose above 70°C, indicating loss of water molecules of crystallization

Table 1. IR spectral data (cm^{-1}) for the complexes.

Complex		$\nu_{C–N}$ thioureide	$\nu_{C–S}$	$\nu_{C=O}$	tmed, 2,2′-bipy, 1,10-phen and oxine	$\nu_{C–N}$ (tertiary)
$[Zn(padtc)_2]$	(**1**)	1490	1011	1772, 1711	–	1395
$[Zn(padtc)_2(tmed)] \cdot C_6H_5CH_3 \cdot 0.5H_2O$	(**2**)	1466	1034, 956	1771, 1711	–	1396
$[Cd(padtc)_2]$	(**3**)	1480	1013, 973	1773, 1713	–	1395
$[Cd(padtc)_2(tmed)] \cdot C_6H_5CH_3 \cdot 0.36H_2O$	(**4**)	1465	1033, 984	1771, 1716	–	1394
$[Hg(padtc)_2] \cdot H_2O$	(**5**)	1472	1019	1773, 1710	–	1394
$[Hg(padtc)_2(2,2'\text{-bipy})] \cdot H_2O$	(**6**)	1456	1020	1773, 1711	1582	1395
$[Hg(padtc)_2(1,10\text{-phen})] \cdot H_2O$	(**7**)	1464	1025	1775, 1710	1619, 1504	1396
$[Hg(padtc)_2(oxine)] \cdot H_2O$	(**8**)	1465	1043	1773, 1713	1618	1395

(experimental loss: 1.80%; theoretically expected: 1.67%). Immediately after loss of water, a single step decomposition step proceeds up to 330°C corresponding to the stabilization of $Hg(NCS)_2$ (experimentally observed residue: 30.5%; theoretically expected: 29.4%), which on further heating leaves a very small residue due to a series of exothermic reactions leading to total evaporation.

All the complexes show almost similar thermal behavior. $[Hg(padtc)_2(2,2'\text{-bipy})] \cdot H_2O$ (**6**) shows loss of 2,2′-bipy (230°C, 12.6%) followed by thermal decay of dithiocarbamate up to 360°C giving $Hg(NCS)_2$ and a small residue of HgS leading to total evaporation as observed for the parent bisdithiocarbamate. Thermal decay of $[Hg(padtc)_2(1,10\text{-phen})] \cdot H_2O$ (**7**) shows initial loss of water (70–130°C, 1.41%); subsequent mass loss led to HgS as final residue. $[Hg(padtc)_2(\text{oxine})] \cdot H_2O$ (**8**) showed a slightly different thermal behavior. Loss of water was observed (62–120°C, 1.5%); further heating led to loss of $C_6H_4(CO_2)N$ (120–160°C, 47.7%). The next step of decomposition corresponds to loss of $[(C_2H_4)NCS_2)]$ (>160–300°C, 23.9%). Subsequent loss of oxine was observed around 300–400°C (11.9%). Above 400°C there was a continuous loss of mass and around 600°C the whole mass evaporated leaving no residue. All the TG analysis showed that the mercury complexes conformed to the proposed molecular formulae and there was total evaporation of the complexes above 600°C.

3.3. *NMR spectral studies*

NMR spectral data of all the compounds are given in table 2 along with splitting patterns. NMR spectra of only **2** and **4** are reported and other compounds were found to be highly insoluble in common organic solvents.

3.3.1. ^{1}H NMR.

^{1}H NMR spectra of **2** showed triplets at 4.21 and 4.04 ppm corresponding to α- and β-CH_2 protons of padtc. In the case of cadmium adduct (**4**), signals were observed at 4.26 and 4.07 ppm as triplets; α- and β-protons adjacent to the electron withdrawing $-(O{=}C)_2-N$ groups appear at higher field. The observed deshielding of the α-protons in all cases [21] is attributed to the release of electrons on nitrogen of NR_2, forcing electron density toward sulfur (or the metal) *via* the thioureide π-system. A shift of electron density toward the metal through the thioureide

Table 2. ^{1}H and ^{13}C NMR spectral data of **2** and **4** (chemical shifts in ppm).

Compound	NMR	Phenyl ring protons/carbons	α-CH_2	β-CH_2	N $^{13}CS_2$ (thioureide)	tmed $-CH_2-$ and $-CH_3$ protons/carbons	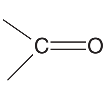
2	^{1}H	7.17–7.83 (m)	4.21(t)	4.04(t)	–	2.26(t)–CH_2–2.04(s)–CH_3	–
	^{13}C	123–133	51.7[b]	34.7[b]	210.9	56.5–CH_2–45.9–CH_3	167.9
4	^{1}H	7.16–7.83 (m)	4.26(t)	4.07(t)	–	2.26(t)–CH_2–1.96(s)–CH_3	–
	^{13}C	123–133	52.6[b]	34.7[b]	211.9	56.0–CH_2–45.4–CH_3	167.9
tmed[a]	^{1}H	–	–		–	2.38(t)–CH_2–2.24(s)–CH_3–	–
	^{13}C	–	–	–	–	57.66–CH_2–45.78–CH_3–	–

[a]Values from Spectral Data Base System.
[b]Values are interchangeable.

bond is more pronounced than a movement of electrons toward the carbonyl, which leads to minimal deshielding of the α-CH_2 protons. The magnitude of deshielding decreases with increase in distance from the metal or the thioureide bond. A change of the central metal [Zn/Cd] does not affect the position of the signals very much as the interaction is mainly electrostatic in nature. In free tmed, methyl protons appear at 2.24(s) ppm and the methylene protons appear at 2.38(t) ppm. As a result of adduct formation, methyl protons of **2** appear at 2.04 ppm and the corresponding methylene protons at 2.26 ppm. The observed marginal shift to lower field of both the signals indicate reduced electron density around nitrogen in tmed as a result of adduct formation. For **4**, a similar trend is observed, 1.96 (methyl) and 2.26 ppm (methylene).

3.3.2. ^{13}C NMR. The most important thioureide ($N^{13}CS_2$) carbon signals for **2** and **4** are at 210.9 and 211.9 ppm. Generally, the extent of deshielding for the thioureide $N^{13}CS_2$ in main group dithiocarbamates is greater in magnitude than those of normal valence state transition metal dithiocarbamates, in line with the observed thioureide carbon chemical shifts of the reported compounds [22]. Chemical shifts of α- and β-CH_2 carbons of **2** are observed at 51.7 and 34.7, respectively, and for the α- and β-CH_2 carbons of **4**, the signals are observed at 52.6 and 34.7 ppm, respectively. The α-carbon signals in **2** and **4** showed a relatively large chemical shift compared to $-CH_2$ because of the proximity of α-CH_2 carbon to $(O{=}C)_2N-$. Both carbonyl carbons in **2** and **4** resonate at 167.9 ppm. The observed small differences in chemical shifts for free tmed, its adducts **2** and **4** (table 2) can be attributed to complexation.

3.4. *Single crystal X-ray structural analysis*

$[Zn(padtc)_2(tmed)] \cdot C_6H_5CH_3 \cdot 0.5H_2O$ (**2**) and $[Cd(padtc)_2(tmed)] \cdot C_6H_5CH_3 \cdot 0.36H_2O$ (**4**) are monomeric. PLUTO plots of **2** and **4** are shown in figures 2 and 3 together with the atom-numbering scheme; PLUTO plots were of better clarity than the ORTEP plots for the two structures. Details of the structure solution are given in table 3. Two formula units are present in the unit cell. From the crystal structures of **2** and **4**, it is clear that zinc and cadmium are six-coordinate with four sulfurs from dithiocarbomates and two nitrogens from tmed. The geometry around the metal ions is a distorted octahedron. In **2**, the short thioureide C–N distance, 1.341(4) Å, indicates that the π-electron density is delocalized over S_2CN and that this bond has strong double bond character. Because of the small bite angle [S–Zn–S = 70.69(4) Å] of the dithiocarbamate and the steric influence of tmed, zinc is in a highly distorted octahedral coordination environment. The distinct asymmetry in Zn–S distances [Zn(1)–S(2) = 2.5189(11) and Zn(1)–S(1) = 2.5415(12) Å] is either due to the steric effect of the bulky methyl groups on tmed or the preference of zinc for four coordination. The bulky methyl groups force a strict packing requirement in the solid state and hence a highly significant asymmetry in Zn–S bonds. However, the indicated asymmetry in Zn–S distances does not manifest itself in C–S distances, which are almost symmetrical [S(1)–C(1) = 1.713(4) and S(2)–C(1) = 1.700(4) Å]. The presence of tmed also affects the S–Zn–S bite angle and Zn–S distances. The Zn–N distances are 2.214(3) and 2.217(3) Å. Bond parameters of the alkyl chain attached to N and the phenyl rings are normal.

In **4**, a similar asymmetry in Cd–S distances is observed [Cd(1)–S(2) = 2.6493(19) and Cd(1)–S(1) = 2.7056(17) Å], due to the steric repulsions of the two dithiocarbamates

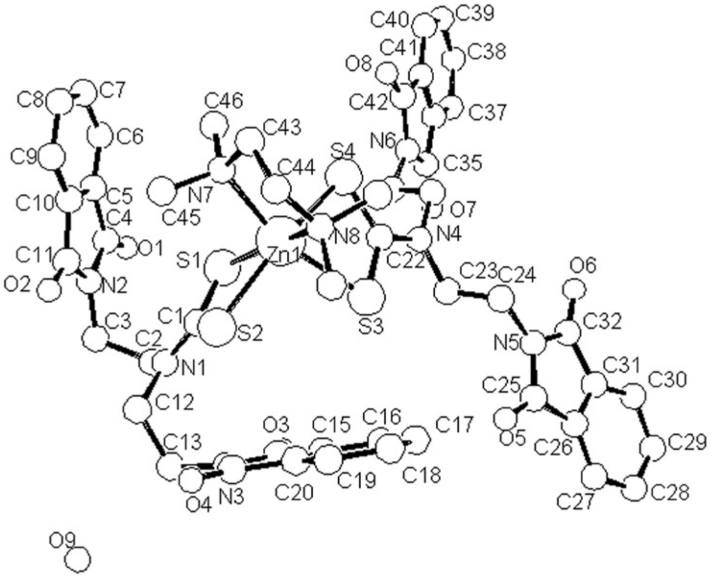

Figure 2. PLUTO plot of **2** (H atoms and toluene molecule are not included).

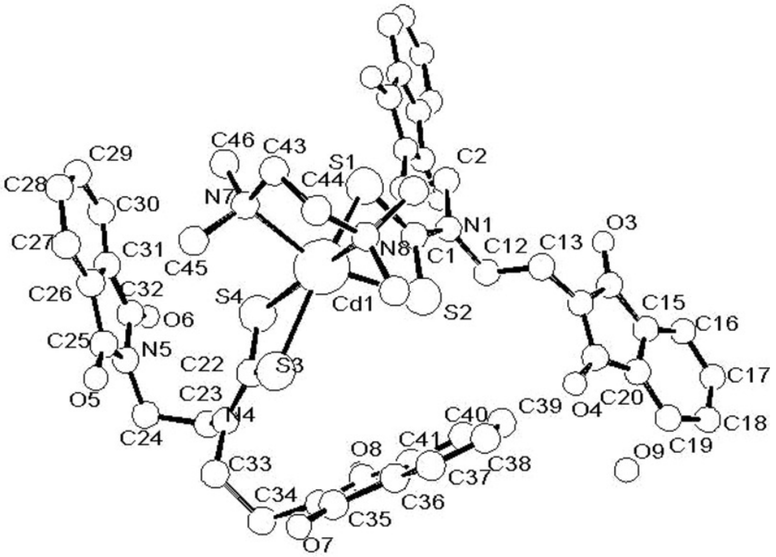

Figure 3. PLUTO plot of **4** (H atoms and toluene molecule are not included).

and tmed. The short thioureide C–N distance [N(1)–C(1) = 1.358(7) Å] indicates that the π-electron density is delocalized over S_2CN. The C–S bond distances [S(1)–C(1) = 1.699(6) and S(2)–C(1) = 1.715(6) Å] are lower than C–S single bond length of 1.81 Å and longer than C=S double bond distance of 1.69 Å. The observed values indicate partial double bond character. The two Cd–N distances associated with tmed are Cd(1)–N(7) = 2.421(5) and Cd(1)–N(8) = 2.406(5) Å, not significantly different.

Table 3. Crystal data, data collection and refinement parameters for **2** and **4**.

Complex	**2**	**4**
Empirical formula	$C_{55}H_{57}N_8O_{8.50}S_4Zn$	$C_{55}H_{56.72}CdN_8O_{8.36}S_4$
Formula weight	1159.7	1204.2
Crystal dimensions (mm)	0.17 × 0.12 × 0.09	0.12 × 0.07 × 0.05
Crystal system	Triclinic	Triclinic
Color	Yellow	Pale yellow
Habit	Prism	Block
Space group	$P\bar{1}$	$P\bar{1}$
Unit cell dimensions (Å, °)		
a	12.4093(11)	12.314(2)
b	14.5615(12)	14.507(2)
c	18.6630(16)	19.101(2)
α	68.7197(16)	109.714(2)
β	88.2412(19)	91.291(2)
γ	64.8915(18)	114.788(2)
Volume (Å^3), Z	2814.9(4), 2	2862.1(7), 2
Calculated density (g cm^{-3})	1.368	1.397
Absorption coefficient (cm^{-1})	0.646	0.587
$F(000)$	1210	1243.2
θ range for data collection (°)	3.8–20.5	3.46–24.88
Diffractometer	Bruker SMART 1000 CCD	Bruker SMART 1000 CCD
Scan type	ω scans	ω^2-q scans
Index ranges	$-14 \le h \le 14$; $-17 \le k \le 17$; $-22 \le l \le 22$	$-14 \le h \le 14$; $-17 \le k \le 17$; $-22 \le l \le 22$
Reflections collected	24,560	22,501
Unique reflections	9547	10,360
Observed reflections $F_o > 4\sigma\ (F_o)$	4010	4673
Weighting scheme	$W = 1/[S^2F_o^2)]$	$W = 1/[S^2(F_o^2) + (0.0253P)^2]$, where $P = (F_o^2 + 2F_c^2)/3$
Number of parameters refined	740	836
Final R, R_w (observed data)	0.0460, 0.0535	0.0723, 0.1042
Goodness-of-fit on F^2	0.903	1.042

The phenyl rings show normal bond parameters and the changes in the bond parameters of tetramethylethylenediamine are due to chelate formation with the metal. To avoid steric interactions with the axial hydrogens, the four methyl groups are equatorially bonded to the two nitrogens in tmed.

A comparison of the bond parameters of **2** and **4** involving zinc and cadmium, respectively, show size effects in M–S, M–N, and S–C–S angles. Both complexes crystallize with one disordered toluene and fractional stoichiometry of water to fill the crystal voids. Toluene was refined by splitting the positions of carbon atoms. Divalent zinc, mercury complexes of pyrrolidinedithiocarbamate have a dinuclear structure with a distorted tetrahedral structure [23, 24]. In this work, two adducts involving bulky dithiocarbamate, padtc, and tmed have been structurally analyzed. The geometry around the metal ions in the adducts is distorted octahedral.

3.5. *Supramolecular aggregation patterns*

Supramolecular interactions stabilize **2** and **4**. Each padtc ligand with six N, four S, and eight O's provide ample opportunities for intermolecular interactions. Table 4 lists

Table 4. Selected bond distances (Å) and angles (°) for **2** and **4**.

2		**4**	
Zn1–N7	2.214(3)	Cd1–N7	2.421(5)
Zn1–N8	2.217(3)	Cd1–N8	2.406(5)
Zn1–S2	2.5189(11)	Cd1-S2	2.6493(19)
Zn1–S3	2.5254(12)	Cd1–S1	2.7056(17)
Zn1–S1	2.5415(12)	Cd1–S3	2.6739(17)
Zn1–S4	2.5685(11)	Cd1–S4	2.6563(18)
S1–C1	1.713(4)	S1–C1	1.699(6)
S2–C1	1.700(4)	S2–C1	1.715(6)
S3–C22	1.700(4)	S3–C22	1.722(6)
S4–C22	1.694(4)	S4–C22	1.709(6)
N1–C1	1.341(4)	N1–C1	1.358(7)
N4–C22	1.358(4)	N1–C2	1.460(7)
N1–C12	1.458(4)	N4–C22	1.355(7)
N7–Zn1–N8	81.72(13)	N8–Cd1–N7	75.7(2)
N7–Zn1–S2	98.29(9)	N8–Cd1–S2	93.64(16)
N8–Zn1–S2	96.86(9)	N8–Cd1–S1	100.80(14)
N7–Zn1–S1	95.77(10)	N7–Cd1–S4	97.72(15)
N8–Zn1–S1	166.90(9)	N8–Cd1–S3	97.97(14)
S2–Zn1–S1	70.69(4)	S2–Cd1–S1	67.61(5)
S3–Zn1–S1	92.80(4)	S4–Cd1–S3	67.62(5)

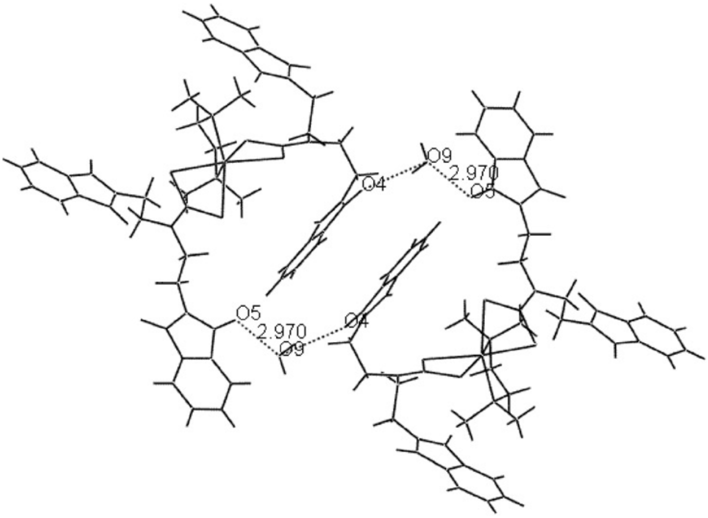

Figure 4. H-bonded supramolecular interactions involving H_2O in **2**.

selected geometric parameters for the zinc and cadmium structures. In [Zn(padtc)$_2$(tmed)], eight oxygens were expected to H bond. Interestingly, the prominent and significant hydrogen bond interaction is observed with water at a distance of 2.246 Å (O(4)···H(91)) as shown in figure 4. H-bond interaction between O(9)···H(17) at 2.710 Å is an interaction which holds the network together. Supramolecular interaction, O(1)···H(19), involving hydrogen of phenyl is observed

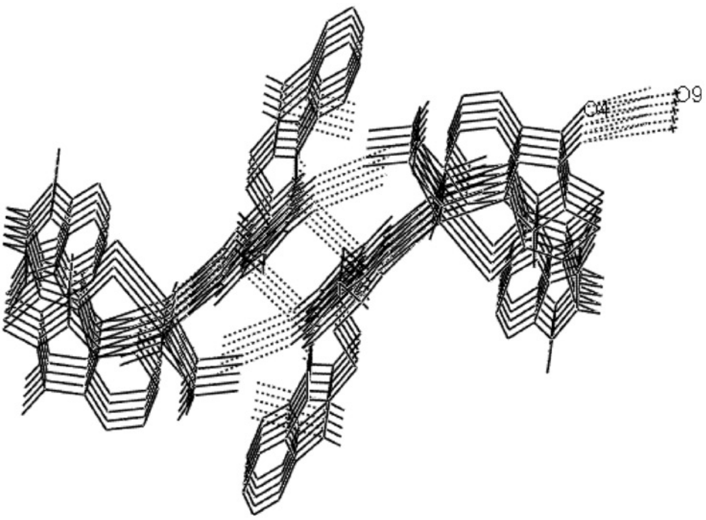

Figure 5. Stacked molecules of **2** and supramolecular interactions.

at a distance of 2.654 Å. A strong O(2)···H(44) interaction involving hydrogen of tmed is observed at 2.314 Å. O(3)···H(2A) and O(3)···H(3A) interactions involving hydrogens of tmed are observed at 2.659 and 2.669 Å, respectively. Interaction between O(6) and H(43B) of tmed shows a reasonably strong hydrogen bond with a distance of 2.585 Å. O(5) and O(7) show little interaction except sterically forced proximity with other atoms of the molecule leading to nonclassical interactions. A strong hydrogen bond is observed between O(8) and H(29) of phenyl intermolecularly at a distance of 2.455 Å. For a stacked molecular arrangement, the supramolecular interactions are shown in figure 5. Toluene exhibits disorder and the positions of carbon atoms are identified by splitting its occupancy and hence its interaction with its neighbors through non-bonded interactions is not analyzed in depth. Interestingly, no S···H non-bonded interaction is observed for the zinc adduct. Distance between two non-bonded Zn's is 13.032 Å. The molecules are stacked along the "*a*"-axis.

In [Cd(padtc)$_2$(tmed)] interaction between O(1)···H(17) of phenyl showed a non-bonded interaction at 2.386 Å, a reasonably strong intermolecular interaction. Interestingly, O(2) shows no short contacts. Two of the oxygens, O(3) and O(5), show supramolecular interactions with H(43A) and H(44B) of tmed at 2.599 and 2.317 Å, respectively. O(4) and O(7) have H-bonded interaction with O(H2) at 2.098 and 2.220 Å. O(8) is involved in two non-bonded interactions in a triangular fashion intramolecularly with H(23A) and H(24A) of the centrosymmetrically related tmed at 2.610 and 2.636 Å. The phthalimide rings are perfectly stacked as shown in figure 6. An interaction between S(1) and H(13B) of the ethyl attached to the phthalimide is observed at 2.953 Å. Similar S···H interactions in bis(diallyldithiocarbamato)zinc(II) have been reported [25, 26]. Bi(III) and As(III) dithiolates also show S···H interactions [13]. The supramolecular interactions strengthen the molecular aggregation. Short non-bonded interactions observed for hydrogens indirectly support their identification

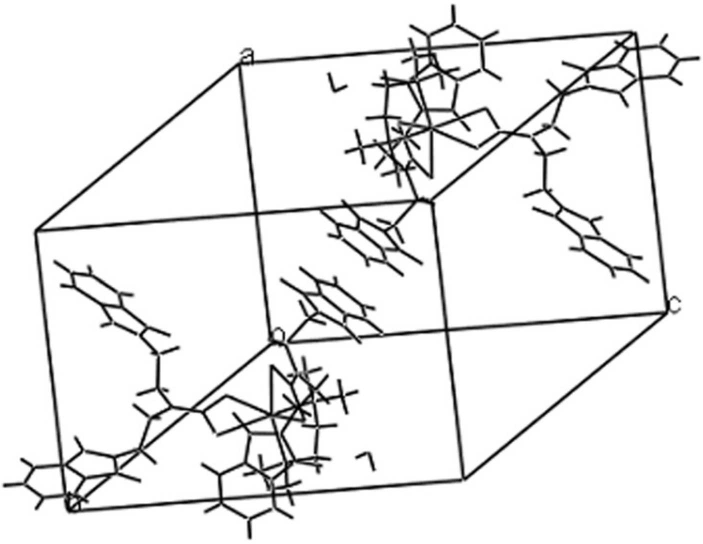

Figure 6. Packing diagram of **4** showing stacking.

through fixed position refinement. The non-bonded Cd···Cd distance is 10.370 Å. The molecular stacking is along the "*a*"-axis of the unit cell. Toluene is disordered and has been refined by splitting the positions of the carbons. Hence, the interactions between the toluene and other atoms are significant but the disorder associated with it prevents the meaningful analysis of the parameters. While the presence of a partial-occupancy water appears to be mandatory to fill a void in the crystal packing, a (partial) water is also supported by the geometry of the site providing a rather consistent environment for O(water)–H···O hydrogen bonds.

C–H···S interactions are often observed in compounds involving metal dithiolates and such an interaction often leads to discernable chains. C–H···S interaction is observed in the Cd complex and not in the Zn complex. In the cadmium compound, non-bonded Cd···Cd distance is shorter than the Zn···Zn distance observed in the zinc analogue, indicating stronger supramolecular forces operating in **4** than **2**.

3.6. *BVS analysis*

The BVS model can be used to determine compatibility between a given coordination model and a particular unknown oxidation state [27, 28]. BVS method is useful in assigning oxidation state of the main group metal in complexes. BVS values are calculated by two procedures [29, 30]. The BVS for zinc in $[Zn(padtc)_2(tmed)] \cdot C_6H_5CH_3 \cdot 0.5(H_2O)$ (**2**) is 1.759 (OK/B) and $[Cd(padtc)_2(tmed)] \cdot C_6H_5CH_3 \cdot 0.36(H_2O)$ (**4**) is 1.9788 (OK/B). These are close to 2.0, the expected valency of the central metal, in **2** and **4**. Relatively lower BVS value for zinc compared to cadmium compound is due to its larger covalent character compared to the cadmium analogue.

Supplementary material

CCDC nos 659327 and 659326 contain the supplementary crystallographic data for **2** and **4**. These data can be obtained free of charge *via* http://www.ccdc.cam.ac.uk/conts/retrieving.html, or from the Cambridge Crystallographic Data Centre, 12 Union Road, Cambridge CB2 1EZ, UK; Fax: (+44) 1223-336-033; or E-mail: deposit@ccdc.cam.ac.uk.

References

[1] J. Nieuwenhuizen, A.W. Ehless, J.G. Haashoot, S.R. Janse, J. Reedijk, J. Baerends. *J. Am. Chem. Soc.*, **121**, 163 (1999).
[2] J.A. McCleverty, S. Gill. *J. Chem. Soc., Dalton Trans.*, 493 (1982).
[3] J.S. Casas, A. Sanchez, J. Bravo, S. Garcia-Fontan, E.E. Castellano, M.M. Jones. *Inorg. Chim. Acta*, **158**, 119 (1989).
[4] M.M. Jones, S.G. Jones. *Inorg. Chim. Acta*, **79**, 288 (1983).
[5] P. Yan, Y. Xie, Y. Qien, X. Liu. *Chem. Commun.*, 1293 (1999).
[6] D.W. Tomlin, T.M. Cooper, D.E. Zelmon, Z. Gebeyehu, J.M. Hughes. *Acta Crystallogr., Sect. C*, **55**, 717 (1999).
[7] P.Ó. Brien, J.R. Walsh, I.M. Watson, M. Motevalli, L. Hendriksen. *J. Chem. Soc., Dalton Trans.*, 2491 (1996).
[8] J. Cheon, D.S. Talaga, J.I. Zink. *J. Am. Chem. Soc.*, **119**, 163 (1997).
[9] M. Bochmann. *Chem. Vap. Deposition*, **2**, 85 (1996).
[10] E.R.T. Tiekink. *Cryst. Eng. Commun.*, **5**, 101 (2003).
[11] R.J. Magee, J.O. Hill. *Rev. Anal. Chem.*, **8**, 5 (1985).
[12] S.P. Huang, K.J. Franz, E.H. Arnold, J. Devenyi, R.H. Fish. *Polyhedron*, **15**, 4241 (1996).
[13] E.R.T. Tiekink. *Cryst. Eng. Commun.*, **8**, 104 (2006).
[14] B. Arul Prakasam, K. Ramalingam, G. Bocelli, A. Cantoni. *Phosphorus, Sulfur and Silicon and the Related Elements*, **184**, 2020 (2009).
[15] Bruker. *SADABS* (*Version 2007/4*), Bruker AXS Inc., Madison, Wisconsin, USA (2008).
[16] A.C.T. North, D.C. Phillips, F.S. Mathews. *Acta Crystallogr., Sect. A*, **24**, 351 (1968).
[17] L.J. Farrugia. *ORTEP-3 for Windows*, University of Glasgow, Scotland, UK (1999).
[18] A.M.A. Hassaan, E.M. Soliman, A.M. El-Roudi. *Polyhedron*, **8**, 925 (1989).
[19] C.P. Sharma, N. Kumar, M.C. Khandpal, S. Chandra, Y.G. Bhide. *J. Inorg. Nucl. Chem.*, **43**, 923 (1981).
[20] C. Petri, G. Tosi, P. Zanini. *J. Mol. Struct.*, **53**, 35 (1979).
[21] M. Saravanan, K. Ramalingam, G. Bocelli, A. Cantoni. *Appl. Organomet. Chem.*, **18**, 103 (2004).
[22] H.L.M. Gaal, J.W. Van Diesveld, F.W. Pijpers, J.G.M. Van Der Lindon. *Inorg. Chem.*, **18**, 3251 (1979).
[23] M. Shahid, T. Ruffer, H. Lang, S.A. Awan, S. Ahmad. *J. Coord. Chem.*, **62**, 440 (2009).
[24] M. Altafa, H.S. Evans, S.S. Batool, A.A. Isab, S. Ahmad, M. Saleem, S.A. Awan, M.A. Shaheen. *J. Coord. Chem.*, **63**, 1176 (2010).
[25] B.F. Ali, K.A. Al-Sou'od, R. Al-Far, Z. Judeh. *Struct. Chem.*, **17**, 423 (2006).
[26] R.E. Benson, C.A. Ellis, C.E. Lewis, E.R.T. Tiekink. *Cryst. Eng. Commun.*, **9**, 930 (2007).
[27] I.D. Brown. *J. Solid State Chem.*, **82**, 122 (1998).
[28] M.H. Whangbo, C.C. Toradi. *Science*, **249**, 1143 (1990).
[29] N.E. Brese, M.Ó. Keeffe. *Acta Crystallogr., Sect. B*, **47**, 192 (1991).
[30] M. Ó'Keeffe, N.E. Brese. *J. Am. Chem. Soc.*, **113**, 3226 (1991).